A recurrent de novo mutation in KCNC1 causes progressive myoclonus epilepsy

Published in final edited form as:
Nat Genet. 2015 January ; 47(1): 39–46. doi:10.1038/ng.3144.

A recurrent *de novo* mutation in *KCNC1* causes progressive myoclonus epilepsy

A full list of authors and affiliations appears at the end of the article.

Abstract

Progressive myoclonus epilepsies (PMEs) are a group of rare, inherited disorders manifesting with action myoclonus, tonic-clonic seizures, and ataxia. We exome-sequenced 84 unrelated PME patients of unknown cause and molecularly solved 26 cases (31%). Remarkably, a recurrent *de novo* mutation c.959G>A (p.Arg320His) in *KCNC1* was identified as a novel major cause for PME. Eleven unrelated exome-sequenced (13%) and two patients in a secondary cohort (7%) had this mutation. *KCNC1* encodes $K_V3.1$, a subunit of the K_V3 voltage-gated K^+ channels, major determinants of high-frequency neuronal firing. Functional analysis of the p.Arg320His mutant channel revealed a dominant-negative loss-of-function effect. Ten patients had pathogenic mutations in known PME-associated genes (*NEU1, NHLRC1, AFG3L2, EPM2A, CLN6, SERPINI1*). Identification of mutations in *PRNP*, *SACS*, and *TBC1D24* expand their phenotypic spectrum to PME. These findings provide important insights into the molecular genetic basis of PME and reveal the role of *de novo* mutations in this disease entity.

Correspondence should be addressed to Anna-Elina Lehesjoki (anna-elina.lehesjoki@helsinki.fi).

Author Contributions

Study design and management: S.F.B., L.M.D., A.P., A.-E.L. *Coordination of the collection of study subjects and clinical data:* S.F.B., K.L.O., M.A.B., A.-E.L. *Subject ascertainment and phenotyping:* S.F.B., K.L.O., L.C., S.F., R.M., E.A., F.A., A.G., P.T., L.L., I.E.S., C.C., A.F., E.F., J.A., A.A., B.B., E.S., M.T., P.R., M.D.K., C.O., D.M.A., B.A.E., A.C., M.L., E.L., V.S., J.M., M.P., A.E., B.K., M.D., R.S.M., R.S., Z.A., B.B.-Z. *Analysis of the exome sequencing data:* M.M., S.Mar. *Sanger sequencing and sequence data analysis, mosaicism analysis:* M.M., M.A.B., T.J., S.E.H., M.S.H. *Interpretation of genetic data:* M.M., S.F.B., L.M.D., A.P., A.-E.L. *Evaluation of the mutation rate in KCNC1:* K.E.S., M.J.D. *Functional analysis and interpretation:* S.Mal., S.P., H.L. *Manuscript writing:* M.M., S.F.B., L.M.D., K.L.O., S.Mal., H.L., A.P., A.-E.L. All authors critically revised the manuscript.

URLs

CADD, http://cadd.gs.washington.edu/; Epilepsy (Lemke *et al*.) and neurodegenerative disease gene panels (accessed Feb 2014), http://www.cegat.de; ClustalX, http://www.clustal.org/clustal2/; Exome Variant Server of NHLBI GO Exome Sequencing Project (accessed Feb 2014), http://evs.gs.washington.edu/EVS/; GATK, http://www.broadinstitute.org/gatk/; The Genotype-Tissue Expression (GTEx) project, http://www.gtexportal.org/; MITOMAP: A Human Mitochondrial Genome Database (accessed Feb 2014), http://www.mitomap.org; NCBI ClinVar, http://www.ncbi.nlm.nih.gov/clinvar/; Online Mendelian Inheritance in Man, OMIM® (accessed Feb 2014), http://omim.org/; Picard, http://picard.sourceforge.net; Primer-Blast, http://www.ncbi.nlm.nih.gov/tools/primer-blast/; Sequencing Initiative Suomi (SISu), http://sisuproject.fi; UCSC Genome Browser, http://genome.ucsc.edu/; UniProt database, http://www.uniprot.org/.

Accession codes

Mutation nomenclatures correspond to the following canonical Ensembl transcripts: *KCNC1*, ENST00000265969.6; *NEU1*, ENST00000375631.4; *NHLRC1*, ENST00000340650.3; *EPM2A*, ENST00000367519.3; *CLN6*, ENST00000249806.5; *AFG3L2*, ENST00000269143.3; *TBC1D24*, ENST00000293970.5; *SACS*, ENST00000382298.3; *SERPINI1*, ENST00000295777.5; *PRNP*, ENST00000379440.4; *SCN1A*, ENST00000303395.4.

The raw aligned sequence reads were submitted to the European Genome-phenome Archive (https://www.ebi.ac.uk/ega/home) by Wellcome Trust Sanger Institute under study accession numbers EGAS00001000048 and EGAS00001000386.

Competing Financial Interests

Authors declare no potential competing financial interests.

Europe PMC Funders Author Manuscripts

PMEs are among the most devastating forms of epilepsy. They are clinically and genetically heterogeneous, characterized by core features of action myoclonus, tonic-clonic seizures, and progressive neurological decline[1]. Most molecularly characterized PMEs are autosomal recessively inherited with rare cases showing autosomal dominant or mitochondrial inheritance[2,3]. Unverricht-Lundborg disease (ULD; OMIM 254800) is the commonest form of PME in most series and an important clinical feature is preservation of cognition[1-3]. ULD is caused by mutations in *CSTB*[4], and mutations in recently discovered genes including *SCARB2*[5,6] and *GOSR2*[7] also contribute to cases of PME with preserved cognition. Other PMEs may have additional features, particularly dementia. PME-associated genes encode a variety of proteins, many of them being associated with endosomal and lysosomal function[8,9], but the associated disease mechanisms are generally poorly understood.

The precise clinical diagnosis of specific forms of PME is challenging due to their genetic heterogeneity, phenotypic similarities and overlap of symptoms with other epileptic and neurodegenerative diseases. In many cases, there are no distinguishing clinical features or biomarkers. Consequently, a substantial proportion of PME cases remain without a molecular diagnosis[3].

Here, we aimed to identify the causative genes for unsolved PME cases by employing exome sequencing in unrelated patients assembled from multiple centers in Europe, North America, Asia, and Australia over a 25-year period. The extent of previous molecular studies varied, but all cases were negative for mutations in the *CSTB* gene and approximately half were negative for *SCARB2* and *GOSR2* mutations. The patient cohort was thus enriched for novel gene findings and potential atypical phenotypes associated with known disease genes.

Results

We exome sequenced 84 unrelated PME cases, of which 70 were sporadic and 14 were from families with pedigrees suggestive of either dominant or recessive inheritance. We therefore analyzed the data seeking pathogenic autosomal recessive or dominant/*de novo*, sex-linked, and mitochondrial DNA (mtDNA) variants (Fig. 1, **Online Methods**). On average 4.15 Gb of sequence was produced within the exome bait regions with an average coverage of 81 reads per nucleotide (Supplementary Table 1). After filtering the raw variant data for possible pathogenic variants, we first analyzed the data for mutations in known PME, epilepsy, or neurodegenerative disease genes followed by analysis for novel genes under both the recessive and dominant/*de novo* models. Analysis of the filtered variant data under the recessive model (Fig. 1a,b) revealed pathogenic or probably pathogenic mutations (see **Online Methods** for classification criteria) in known disease-causing genes in 12 patients. Analysis under the dominant/*de novo* model (Fig. 1a,b) led to discovery of a novel PME-associated gene, *KCNC1*, with, remarkably, the same recurrent *de novo* mutation in 11 patients and, in addition, revealed pathogenic mutations in known disease genes in three patients. We did not identify any obvious pathogenic mutations in mtDNA. In total, we identified pathogenic or probably pathogenic mutations in 26 of 84 cases (31.0%).

Identification of a recurrent mutation in *KCNC1*

To identify novel pathogenic mutations under the dominant/*de novo* model, we analyzed the data for potentially deleterious heterozygous variants absent in three variant databases. In addition, we did not consider variants in dbSNP except for those with a clinical association in the ClinVar database.

The highest number of novel heterozygous variants occurred in *KCNC1* together with *TTN* (Supplementary Table 2). *TTN* encodes a large muscle protein and has a high mutational load[10] due to its large coding region and was thus not considered further. We identified 11 (13.1%) unrelated patients with a novel heterozygous c.959G>A mutation (Supplementary Fig. 1; see **Accession codes** for the transcript IDs) in *KCNC1* encoding the potassium voltage-gated channel (K_V) subfamily C member 1 (KCNC1, also known as K_V3.1). The c.959G>A mutation causes substitution of histidine for arginine at codon 320 of the K_V3.1 protein (p.Arg320His).

In all 11 cases, the mutation was confirmed by Sanger sequencing. Parents of all c.959G>A positive patients were unaffected and segregation analysis in eight patients where both parental DNA samples were available showed that in each case the mutation occurred *de novo* (Fig. 2a and Supplementary Fig. 2). Genotyping a set of microsatellite markers in five trios with sufficient DNA available confirmed that the pedigrees were correct. One of the index patients (PME84-1) with the c.959G>A mutation has an affected sibling and two affected children, who are also each heterozygous for the mutation (Fig. 2a). The parents of PME84-1 and her unaffected brother were both negative for the mutation. The presence of two mutation-positive and clinically affected children from mutation-negative unaffected parents suggests the occurrence of mosaicism in one of the parents. A restriction fragment length assay designed to detect both the normal and mutant alleles was carried out on the peripheral blood DNA from both parents but showed no indication of mosaicism (data not shown).

We screened the *KCNC1* c.959G>A mutation in a secondary cohort of 28 PME patients and identified two (7.1%) additional unrelated cases heterozygous for the mutation. Sanger sequencing of the available parental samples of one of these patients confirmed *de novo* occurrence of the mutation (Fig. 2a). Together, we identified 16 patients (13 unrelated) with the c.959G>A mutation. We did not identify any other mutations in *KCNC1* in the exome data. As exon 1 was not sufficiently covered, we Sanger sequenced it in the 73 exome-sequenced c.959G>A negative patients, but no potentially deleterious variants were found.

The c.959G>A mutation in *KCNC1* affects a highly evolutionarily conserved arginine residue in segment S4 constituting the main voltage-sensing domain of the channel (Fig. 2b,c). The mutation is predicted to be deleterious by all four *in silico* methods used (Supplementary Table 3).

To assess the frequency of PME due to *KCNC1* c.959G>A, we used a newly published mutational model[10], which takes into account both the local sequence context of mutation site and regional factors such as divergence between humans and macaques, to estimate the rate of this specific mutation. A rate of 1.75×10^{-7} per person was obtained, indicating that

the mutation should occur in 1/5,700,000 conceptions. Additionally, we examined three other potential mutations encoding changes of the conserved voltage-sensing arginines to histidines in segment S4 of $K_V3.1$ (p.Arg311His, p.Arg314His, p.Arg317His). Given that the sequence context of the four potential mutations is the same (they all occur in highly mutable CGC codons), the same estimated rate applied to all of them. If all four caused PME with equal penetrance, the probability of seeing only one of four possible mutations in 13 of 13 independent cases is $P = 4 \times (1/4)^{13} = 6.0 \times 10^{-8}$ strongly suggesting the effect of p.Arg320His is surprisingly specific for PME.

Functional analysis of p.Arg320His in $K_V3.1$ channel

To assess the effects of the p.Arg320His substitution on channel function, we used the *Xenopus laevis* oocyte expression system and automated two-electrode voltage clamp. Potassium currents were recorded from oocytes injected with identical amounts of wild-type or mutant cRNA of the human $K_V3.1$ channel. Whereas the wild-type channel produced robust currents upon membrane depolarization, the currents observed with the mutant channel were barely detectable (Fig. 3a,b). A western blot analysis using an antibody to DDK-tag revealed similar protein levels in total lysates of oocytes expressing wild-type or mutant subunits, indicating that the mutant protein has a similar stability as the wild-type (Fig. 3c). To examine for a possible interaction of mutant with wild-type subunits, we co-expressed them in a 1:1 ratio. These experiments showed an approximately 80% reduction in the expected current amplitude recorded at +60 mV, indicating a dominant-negative effect (Fig. 3d,e). The diminished currents produced by the combination of mutant and wild-type subunits revealed altered gating properties, with a significant hyperpolarizing shift of the activation curve (Fig. 3f).

The clinical phenotype of patients with the *KCNC1* mutation

We obtained detailed clinical data for 15 of the 16 *KCNC1* mutation-positive patients (Table 1). Their clinical phenotype was similar and, at disease onset, resembled classic ULD. On a background of usually normal development, the first symptom in the majority of patients was myoclonus (sometimes reported as tremor) at ages of 6–14 years. Ataxia developed early in one patient (PME17-1) but otherwise it was overshadowed by myoclonus as the major motor impediment. There were infrequent tonic-clonic seizures in all patients. During adolescence myoclonus generally became very severe, limiting ambulation; a walking aid or wheelchair was needed by mid to late teens. Learning disability prior to seizure onset was noted in some cases; in particular the nuclear family of PME84-1. There was mild cognitive decline in seven subjects in early adolescence, but this was difficult to quantitate due to the severe motor disability. Early death was not observed. Electroencephalogram recordings showed generalized epileptiform discharges with photosensitivity in some cases. MRI scans had no specific features; and were regarded as normal or showed cerebellar atrophy. The clinical picture in the family with four affected members (PME84) was milder; the two older sisters were ambulant in the fourth decade. Similarly, the secondary cohort case 1 had a less severe course than the majority of cases.

Mutations in known disease genes

Analysis for mutations in known PME, epilepsy, and neurodegenerative disease genes revealed either pathogenic or probably pathogenic mutations in 15 out of the 84 exome sequenced patients (Table 2; see Supplementary Table 4 for clinical details as well as summaries of the genetic findings, Supplementary Fig. 3 for pedigrees with segregation data, and Supplementary Figs. 4 and 5 for conservation of the novel mutation sites). These fell into three groups.

First, ten patients had recessively inherited or a *de novo* heterozygous mutation in established PME genes, seven with atypical clinical presentations. The ten comprised three cases of Lafora disease (*NHLRC1* and *EPM2A*), three cases of sialidosis (*NEU1*), and one of neuronal ceroid lipofuscinosis (*CLN6*), all well-recognized PME genes. Two Italian cases, not known to be related, had the same novel homozygous missense *AFG3L2* mutation (c.1875G>A, p.Met625Ile) in the proteolytic domain of the protein (Supplementary Fig. 4e). Exome data showed that they shared a ~1.75 megabase run of identical homozygous polymorphisms flanking the mutation, indicating that the mutation is identical by descent. The tenth case had a *de novo* previously described[11] pathogenic heterozygous missense mutation (c.1175G>A, p.Gly392Glu) in the *SERPINI1* coding neuroserpin. Mutations in both *AFG3L2* and *SERPINI1* are very rare known causes of PME.

Second, four patients had mutations in known genes where PME has not been reported as a key part of the presentation. One case with an adult-onset PME and a father who had died of a similar disease was found to have a previously described[12] pathogenic heterozygous missense mutation (c.305C>T, p.Pro102Leu) in the *PRNP* gene encoding prion protein. The mutation is a known cause of Gerstmann-Sträussler-Scheinker disease, one of the inherited prion diseases. Two unrelated patients had probably pathogenic, rare compound heterozygous missense mutations in the *SACS* gene (c.8393C>A, p.Pro2798Gln in both patients; c.1373C>T, p.Thr458Ile and c.2996T>C, p.Ile999Thr in one patient each). Two of the substitutions (p.Thr458Ile, p.Pro2798Gln) have been reported in spastic ataxia patients[13-15]. One patient had a novel probably pathogenic, homozygous missense mutation (c.1079G>T, p.Arg360Leu) in *TBC1D24*, where recessive mutations cause variable neurological disorders including familial infantile myoclonic epilepsy[16-20].

Third, in one patient we identified a previously seen[21] pathogenic heterozygous mutation (c.677C>T, p.Thr226Met) in *SCN1A*, the major gene underlying severe myoclonic epilepsy of infancy (Dravet syndrome)[22]. The eventual clinical evolution of this case was typical of Dravet syndrome, and not that of PME. Initial consideration of PME as a clinical diagnosis was due to the predominence of myoclonic seizures in the early disease course.

All variants passing the filtering in the known disease genes, including the ones not considered pathogenic or probably pathogenic, are listed in Supplementary Tables 5 (recessive) and 6 (dominant/*de novo*).

Search for additional novel genes

We analyzed the exome dataset for potential novel PME genes, other than *KCNC1*, using both recessive and dominant/*de novo* models. We did not identify other likely novel genes

using our criteria of observing putative mutations in a gene in at least two unsolved patients under the recessive model or in at least four patients using the dominant/*de novo* model (Supplementary Note, Supplementary Tables 2 and 7). However, genes of interest in single cases that would warrant further exploration include *ALG10* and *APOA1BP*, which harbor homozygous loss-of-function mutations (Supplementary Table 8).

Discussion

Using an exome sequencing approach in a clinically heterogeneous cohort of 84 unrelated PME patients without a specific cause, we reached a genetic diagnosis in 31% of the cases. Importantly, we identified a recurrent mutation in *KCNC1* as a novel cause of PME explaining a substantial proportion of cases. *KCNC1* encodes $K_V3.1$ functioning as a highly conserved[23] K^+ channel subunit of the K_V3 subfamily of voltage-gated tetrameric K^+ channels. While *KCNC1* mutations have not been associated with human disease to date, autosomal dominantly inherited or *de novo* missense mutations in *KCNC3* ($K_V3.3$) cause spinocerebellar ataxia[24-27].

K_V3 channel subunits consist of six membrane-spanning segments (S1–S6), have overlapping expression patterns, and can form heterotetramers[28]. S4 constitutes the main voltage-sensor where specific positively-charged arginines contribute to the gating charge[29,30].

Electrophysiological analysis showed that the PME-causing p.Arg320His substitution, which affects one of the voltage-sensing residues, has a prominent loss of function with a dominant-negative effect on wild-type $K_V3.1$ channels. We also observed altered gating properties but the physiological consequence of this finding is questionable as its overall contribution on $K_V3.1$-mediated current is minor. Similar biophysical properties have been reported for an ataxia-causing alteration in $K_V3.3$, p.Arg423His[31], occurring in the position analogous to p.Arg320His in $K_V3.1$. Mutations affecting positively charged residues in S4 of voltage-gated cation channels may contribute to pathogenicity by generating leak currents through the gating pore[32]. For example, in *Shaker* K_V channel the change analogous to $K_V3.1$ p.Arg320His increases proton permeability[33]. However, gating pore currents are not detectable in the analogous $K_V3.3$ mutant[31], questioning the importance of the phenomenon in the context of $K_V3.1$. Given the ability of K_V3 subunits to form heterotetramers, the dominant-negative p.Arg320His in $K_V3.1$ is likely to disrupt all K_V3-mediated currents of the neurons in which it is expressed. Reflecting functional redundancy, *Kcnc1* and *Kcnc3* knockout mice have relatively mild phenotypes, whereas double mutant mice show myoclonus, tremor, and gait ataxia[34-36]. Thus, the dominant-negative $K_V3.1$ and $K_V3.3$ patient mutations seem to have an effect comparable to the double knockout.

The K_V3 subfamily is distinguished from other K_V channels by showing a more positively shifted voltage-dependent activation and faster activation and deactivation rates. This makes K_V3 channels major determinants of high-frequency firing in several types of central nervous system (CNS) neurons[28]. Studies using mutant or pharmacologically suppressed K_V3 channels have demonstrated that loss of K_V3 function disrupts firing properties of fast-spiking neurons[28,37,38], impacts neurotransmitter release[28,39], and induces cell death[40]. The

expression of $K_V3.1$ is limited to the CNS with the exception of a subpopulation of T lymphocytes[41,42]. It is preferentially expressed in specific subsets of fast-spiking neurons with prominent expression in inhibitory GABAergic interneurons[28,41]. Therefore it is likely that the p.Arg320His substitution in $K_V3.1$ results in disinhibition due to impaired firing of fast-spiking GABAergic interneurons. This mechanism is likely to contribute particularly to myoclonus and tonic-clonic seizures. Furthermore, dysfunction and/or degeneration of cerebellar neurons, where $K_V3.1$ is expressed[41], is likely to contribute to the motor impairment. Modulation of K_V3 channel function may provide a possibility for pharmacological intervention in *KCNC1* patients. However, while drugs with anticonvulsant effects activating other K_V channels exist[43], there is no activator of K_V3 channels currently available.

The initial clinical presentation and evolution of ULD[44] and the disorder in patients with the *KCNC1* mutation, designated here as “MEAK” (Myoclonus Epilepsy and Ataxia due to Potassium channel mutation), are similar. They have overlapping age of onset and moderate to severe incapacitating myoclonus, infrequent tonic-clonic seizures, and mild if any cognitive decline. Differences emerge as the clinical course for MEAK is generally more severe. ULD is caused by mutations in *CSTB* encoding cystatin B implicated in oxidative stress and inflammation[45,46]. Evidence from the mouse model for ULD suggests that altered GABAergic signaling contributes to the latent hyperexcitability[47,48], implying a possible convergent pathway for ULD and MEAK.

The recurrence of the *KCNC1* mutation is likely due to its location in a CpG dinucleotide, which are mutation hotspots[49]. We estimated that the mutation occurs in 1/5,700,000 conceptions, thus potentially affecting hundreds of patients globally. Observation of four *KCNC1* patients ascertained in a multicenter clinical collaboration[3] in Italy supports this estimate assuming that probably not all existing cases were ascertained, and that the mutation may reduce lifespan. We did not observe any other mutations in *KCNC1*, which is among the top 1% most constrained genes[10]. For example, the estimated mutation rate of the three other potential arginine to histidine substitutions affecting the voltage-sensing residues is equal to p.Arg320His and thus should have been observed in our cohort if the phenotypic consequence was the same. This suggests that Arg320 is biophysically special. Indeed, codon specific consequences of S4 mutations have been demonstrated, for example, in $K_V3.3$[31].

Identification of mutations in previously established disease genes expands the phenotypic and genotypic spectrum of PME. Highlighting the utility of exome sequencing as a diagnostic tool in a heterogeneous patient cohort previously subjected to molecular analyses, we identified pathogenic mutations in known PME genes in ten individuals, of whom the majority had atypical symptoms (Supplementary Note and Supplementary Table 4). Importantly, we identified mutations in three known disease genes (*PRNP, SACS, TBC1D24*), where PME has not been appreciated as part of the clinical spectrum. These cases are discussed in Supplementary Note. The majority of all solved cases also had variants in other known disease genes (Supplementary Tables 5 and 6). These variants, however, did not fulfill our criteria for pathogenicity. It is possible that they modify the clinical outcome, thus contributing to some atypical presentations.

The genetic basis remained unknown in over two thirds of cases. Besides *KCNC1*, there were no other novel PME genes definitively identified (Supplementary Note and Supplementary Tables 2 and 7), however, of the nine genes with homozygous loss-of-function mutations in single patients some are interesting candidates (Supplementary Table 8). In light of establishing *de novo* mutations as an important cause of PME, exome sequencing in trio setting could be pursued to further dissect this heterogeneous cohort. Also, the role of CNVs and epistatic mutations in PMEs should be assessed. Our findings, especially the discovery of MEAK, will aid in molecular diagnostics and potential therapeutic interventions in PME and the exome data will facilitate further gene identification.

Online Methods

Study subjects

The cohort consisted of 84 unrelated patients with a clinical presentation of PME, collected from multiple centers in Europe, North America, Asia, and Australia over a 25-year period for molecular study, where a specific diagnosis had not hitherto been made. Seventy-three patients were of European origin, seven of Western Asian, three of Southern Asian, and one of Chinese. The extent of previous molecular investigations varied; mutations in the *CSTB* gene had been excluded in all and 43 patients were tested negative for mutations in *SCARB2* and 39 negative for *GOSR2*. A variable set of other genes was also screened in some patients. Informed consent for DNA analysis was obtained from patients in line with local institutional review board requirements at time of collection. Family members, when available, were recruited for segregation analysis done by Sanger sequencing.

Seventy cases were sporadic. Three probands had either an affected parent or affected offspring. Ten probands had at least one affected sibling and one had an affected cousin with known parental consanguinity. Fifteen of the patients were reported to be the result of a consanguineous union. Based on inbreeding coefficients obtained by FEstim[56] the number is eighteen. No cryptic relatedness (PIHAT > 0.05) between patients was detected by Plink[57] IBD analysis.

A secondary cohort of 28 cases with PME or possible PME was Sanger sequenced for the *KCNC1* recurrent mutation. These cases were excluded from our original cohort for exome sequencing due to insufficient DNA or inadequate clinical data.

Exome sequencing

Exome sequencing was carried out at the Wellcome Trust Sanger Institute (Hinxton, Cambridge, UK). Genomic DNA (approximately 1 μg) extracted from peripheral blood for each sample was fragmented to an average size of 150 bp and subjected to DNA library creation using established Illumina paired-end protocols. Adapter-ligated libraries were amplified and indexed via PCR. A portion of each library was used to create an equimolar pool comprising 4–8 indexed libraries. Each pool was hybridized to SureSelect Human All Exon 50Mb V3 RNA baits (Agilent Technologies) and sequence targets were captured and amplified in accordance with manufacturer's recommendations. Enriched libraries were

subjected to 75 base paired-end sequencing (HiSeq 2000; Illumina) following manufacturer's instructions. Each pool of indexed samples was sequenced twice on two different flow cells.

Sequence read alignment and processing

Alignment of the sequenced DNA fragments to Human Reference Genome was performed using the Burrows-Wheeler Alignment Tool (BWA)[58]. The reference sequence used was the 1000 Genomes Phase II reference (hs37d5) which is based on GRCh37 and consists of chromosomes 1–22, X, Y, as well as mitochondrial genome (rCRS mitochondrial sequence NC_012920), unlocalized and unplaced contigs, Human herpesvirus 4 type 1 (NC_007605), and decoy sequences derived from HuRef, Human Bac and Fosmid clones and NA12878.

Duplicate reads were marked using the Picard toolkit. Sequence reads were further processed using GATK software (version 2.8.1)[59,60] based on GATK Best Practices. Specifically, local realignment was performed around known insertion or deletion (indel) locations, and base quality scores were re-calibrated.

Variant calling

Single nucleotide variants (SNVs) and indels were called for all exomes jointly using GATK HaplotypeCaller. Called variants with quality score >30 were accepted. Variant quality scores of the PME exomes were recalibrated jointly with GATK VariantRecalibrator. HapMap 3.3 and Omni 2.5M SNP chip array from 1000 genomes project were used as truth sites training resources in variant quality score recalibration (VQSR) of SNVs. 'Mills and 1000 genomes gold standard' indels were used as truth sites in indel VQSR. A truth sensitivity cutoff of 99.0% was used for both SNVs and indels. Additional filtering was applied to exclude variant sites where >80% of the samples have a <5× read depth. Individual variant calls with a read depth below 5× were excluded.

Variant filtering under recessive and dominant/*de novo* inheritance models

Reflecting the different possible inheritance patterns of the underlying mutations in the study subjects, we aimed to identify autosomal or sex-linked recessive and dominant (including *de novo*) mutations as well as pathogenic changes in the mitochondrial genome (Fig. 1). We considered coding variants with the following Variant Effect Predictor[61] (Ensembl release 75) annotated variant consequences based on Sequence Ontology nomenclature: missense variant, initiator codon variant, splice donor or acceptor variant, stop lost, stop gained, inframe insertion or deletion (inframe indels in tandem repeat regions[62] obtained from UCSC Genome Browser[63] were excluded), and frameshift variant. If there were multiple Ensembl gene transcripts overlapping the variant site, the transcript having the most severe consequence annotation for the variant was selected while prioritizing Ensembl database canonical transcripts. Only variants within the genes included in the December 2013 version (release 15) of Consensus CDS (CCDS) project, implemented in Ensembl release 75, were considered. To exclude likely benign amino acid changes, missense variants were considered only if two or more of the four *in silico* methods predicted the variant to be deleterious: CADD[64] (PHRED-like scaled C-score >15, which is a suggested threshold for the deleteriousness by the authors), PolyPhen-2 HumVar[65]

("possibly" or "probably damaging"), SIFT[66] ("deleterious"), MutationTaster[67] ("disease causing", the MutationTaster prediction scores were obtained using dbNSFP[68] and correspond to the converted score suggested by the authors). In rare cases, when not all of the four prediction methods could be applied, we accepted missense mutations predicted to be deleterious by at least 50% of the available methods. We also analyzed the exome data using only CADD to evaluate the deleteriousness of silent or noncoding mutations (Supplementary Note).

In the recessive filtering, we included homozygous, hemizygous, or compound heterozygous variants with allele frequencies <1% in the three following variant databases: 1092 exomes from the phase I release of the 1000 genomes project[69], the 6503 exomes of the Exome Variant Server (EVS) NHLBI GO Exome Sequencing Project (version 0.0.25), and 3268 Finnish exomes (Sequencing Initiative Suomi project, SISu; only autosomal SNVs, epilepsy patients removed). Variants present as homozygous or hemizygous in any of the three variant databases were excluded. As we did not exome sequence parental samples, we used three methods for phasing genotypes to facilitate identification of compound heterozygous variants. First, physical phasing of SNV calls, based on the presence of heterozygous variants in the same sequencing reads, was performed using GATK ReadBackedPhasing. Since ReadBackedPhasing method handles SNVs only, heterozygous indels present in the same sequencing reads were removed manually. Second, to detect rare variants segregating together in populations (likely to be inherited from one parent only), Beagle[70] was applied to phase genotypes using 1000 genomes phase I data as a reference. Third, we used genotype information from the 3268 Finnish exomes to detect heterozygous variants likely to be in the same allele. After filtering the variant data using recessive hypothesis prior to taking advantage of the phasing information, we visualized the sequencing reads surrounding the variants passing the filtering using Integrative genomics viewer[71] (IGV) to detect likely false positive calls raising mainly within segmental duplication regions where mapping of reads is more challenging. As a technical comparison set in variant visualization, we used 43 in-house exomes, which had been processed in the same sequencing, read processing and variant calling pipelines as exomes in this study. After excluding low quality variants, we implemented the phasing information to the cleaned data and repeated the recessive filtering.

In the dominant/*de novo* filtering strategy, we assumed full penetrance of the mutations and, since the great majority of patients have disease onset before adulthood (10/84 cases with onset at 18 years or later, maximum onset at 26 years), we included heterozygous variants absent from the three variant databases. Additionally, dbSNP build 138 variants were excluded except those with clinical association in NCBI ClinVar. After applying the filtering criteria, we excluded low quality variants based on IGV visualization of sequencing reads as described in the filtering of recessive variants.

Analysis of filtered variant data under recessive and dominant/*de novo* strategies

The exome data were analyzed both for variants in genes previously associated with PME, epilepsy and/or neurodegenerative disorders and for variants in novel genes. The association of genes to Mendelian diseases was annotated based on the Online Mendelian Inheritance in

Man, OMIM® database[72]. Additionally, genes involved in monogenic forms of epilepsies and neurodegenerative diseases were retrieved based on diagnostic panels developed by Lemke and colleagues[73]. Genes involved in PME were also retrieved from literature.

To identify novel recessive or dominant/*de novo* genetic causes, genes with variants surviving the filtering strategy were ranked based on the number of PME patients with variants in the gene. Genes that are highly polymorphic in human populations and thus are likely to rank high in the data analysis only due to their high and benign mutational load were given less priority if at least one of the following criteria was fulfilled: 1) the gene has a Residual Variation Intolerance Score (RVIS)[74] (estimates the toleration of genes for functional variation) in the most tolerant 10th percentile (this criteria used only in dominant/*de novo* model) and 2) gene was identified as hyperpolymorphic by Fuentes Fajardo and colleagues[75]. Other measures used in prioritization of candidate genes and variants were known disease association, function (Uniprot database[76] and literature) and expression pattern (GTEx database[42] and literature) of the gene.

Analysis of mitochondrial DNA variants

Since PME may also be caused by mutations in the mitochondrial genome[77], we analyzed the mtDNA for possible disease-associated mutations. Even though mtDNA is not included in the SureSelect exome capture kit, we obtained an average of 32.7× sequencing coverage per sample in the mitochondrial genome, due to the abundance of mitochondrial DNA in the cells. We called mtDNA variants using GATK UnifiedGenotyper. At the sites for the most common reported mutations associated with diseases showing myoclonus as part of the clinical presentation, namely myoclonic epilepsy with ragged red fibers (MERRF) and mitochondrial encephalomyopathy, lactic acidosis, and stroke-like episodes (MELAS), the average coverage was at least 24.8×. We searched for novel mitochondrial mutations by excluding known mtDNA polymorphisms in the MITOMAP database. The same database was also used to obtain positions for known disease-associated mtDNA mutations.

Classification criteria for mutations in known disease genes as well as for novel disease genes

We used a three-tier scale to classify mutations passing the variant filtering in known PME, epilepsy, or neurodegenerative disease genes: 1) pathogenic, 2) probably pathogenic, and 3) unlikely pathogenic. The classification criteria were the following.

Pathogenic—Mutation is in a known PME gene, i.e., where mutations cause a disease with PME as a key part of the presentation, or mutation is in a known epilepsy or neurodegenerative disease gene and the mutation has previously been reported as pathogenic and the phenotype of the patient is compatible with the previous cases. In addition, mutations were required to occur in a conserved domain where other pathogenic mutations have previously been reported. Segregation data, when available, had to comply with the expected inheritance in the family and the mode of inheritance had to concur with previously reported cases. If no segregation data were available, the phenotype had to present substantial overlap with previously reported cases, and in the case of previously

Europe PMC Funders Author Manuscripts

reported pathogenic compound heterozygous mutations, they should not be occurring in *cis* in the original reports.

Probably pathogenic—Mutations occur in only one patient in a previously established disease gene with phenotypic overlap with PME or mutations occur in two or more patients in a gene with a previously established association to neurological disease, with little overlap with PME. In addition, mutations are required to occur in a conserved domain where other pathogenic mutations have been reported previously. Segregation data of the mutations had to comply with the expected inheritance in the family and the mode of inheritance had to concur with previously reported cases.

Unlikely pathogenic—Mutations not fulfilling the above listed criteria.

To consider novel disease genes as candidates for PME, we required them to harbor mutations in at least two patients in the recessive variant filtering strategy and in at least four patients in the dominant/*de novo* strategy. The higher threshold in the dominant/*de novo* strategy was set to limit the number of candidates to a feasible level to do follow-up, as exome variant data of the parents was not available for filtering inherited variants in data analysis.

Variant validation and segregation analysis

Candidate mutations in the known and novel disease genes were confirmed and segregation of the variants was analyzed, where DNA from parents or siblings was available, by bidirectional Sanger sequencing (ABI BigDye 3.1, Applied Biosystems) on ABI 3730xl DNA Analyzer. Primers (available from authors upon request) were designed with Primer-Blast[78]. The sequences were analyzed using Sequencher (Gene Codes Corporation) and illustrated using 4Peaks (Nucleobytes Inc.). Evaluation of the quality of sequence reads over the recurrent c.959G>A mutation in *KCNC1* is described in Supplementary Note.

Parental testing of the cases with the c.959G>A mutation in *KCNC1*

Parental testing was carried out for five cases (those with sufficient amount of parental DNA available) with the *de novo* c.959G>A mutation in *KCNC1* mutation to exclude false paternity and inadvertent sample substitution. Biparental testing was performed using twelve highly polymorphic microsatellite markers: *D3S3680*, *D4S418*, *D6S289*, *D7S2560*, *D8S281*, *D13S175*, *D13S221*, *D15S117*, *D19S1150*, *DXS1113*, *DXS1036*, and *DXS7423*. PCRs were done using the Qiagen Multiplex PCR kit according to the manufacturer's instructions. The reverse primer of each pair was labeled with either HEX or FAM. Products were analyzed on an ABI 3131 Genetic Analyzer.

Analysis of parental mosaicism of c.959G>A mutation in *KCNC1* in PME84-1 family

The *KCNC1* exon 2 PCR product was amplified using the same primers and conditions as for sequencing and 10 μl of PCR reaction was digested with 2 units of *Hpy*CH4V (New England Biolabs) for 2 hours at 37°C under the conditions recommended by the manufacturer. Fragments were visualized by electrophoresis of 10 μl of the digest on a 2%

agarose gel in TBE. Gels were stained with RedSafe™ (INtRON Biotechnology). PCRs and digests were performed in duplicate.

Evaluation of the expected rate of mutations encoding arginine to histidine changes in the S4 segment of $K_V3.1$

The expected rate of the four possible mutations encoding arginine to histidine changes (CGC>CAC) in the voltage-sensing arginine residues of the $K_V3.1$ S4 segment (p.Arg311His, p.Arg314His, p.Arg317His, p.Arg320His, see Fig. 2b,c) was established using a recently developed statistical framework[10], which takes into account both the local sequence context of mutation site and regional factors such as divergence between humans and macaques.

Functional analysis of p.Arg320His substitution in $K_V3.1$

Mutagenesis and RNA preparation—We used the Quick Change kit (Stratagene) to engineer the missense mutation c.959G>A (p.Arg320His) in the human *KCNC1* cDNA (NM_004976, this construct corresponds to the $K_V3.1a$ isoform (511 aa), which has a shorter cytoplasmic C-terminal domain but identical biophysical properties compared to the longer $K_V3.1b$ (585 aa) isoform[79]) cloned in a pCMV-Entry vector obtained from OriGene Technologies. This clone contains a C-terminal Myc-DDK-tag. Insertion of the mutation was confirmed and additional mutations excluded by Sanger sequencing. Primers are available upon request. cRNA was prepared using the T7 mMessage mMachine kit from Ambion.

Oocyte preparation and injection—The use of animals and all experimental procedures were approved by local authorities (Regierungspraesidium Tübingen, Tübingen, Germany). Extracted ovary pieces (*Xenopus laevis*) obtained from the Institute of Physiology I, Tübingen were treated with collagenase (1 mg ml^{-1} of type CLS II collagenase, Biochrom KG) in OR-2 solution (mM: 82.5 NaCl, 2.5 KCl, 1 $MgCl_2$ and 5 Hepes, pH 7.6), followed by thorough washing and storing at 16 °C in Barth solution (mM: 88 NaCl, 2.4 $NaHCO_3$, 1 KCl, 0.33 $Ca(NO_3)_2$, 0.41 $CaCl_2$, 0.82 $MgSO_4$ and 5 Tris/HCl, pH 7.4 with NaOH) supplemented with 50 μg ml^{-1} gentamicin (Biochrom KG). The equal volumes (50 nl) of cRNAs with the concentrations adjusted to 2 μg $μl^{-1}$ were injected using Robooinject® (Multi Channel Systems) in the same batch of oocytes plated in 96 well-plates. Recordings were performed in parallel at days 2–3 after injection. Amplitudes of interest for all currents recorded on the same day were normalized to the mean value obtained for the $K_V3.1$ wild-type on that day, so that the normalized data from different experiments could be pooled.

Automated oocyte two-microelectrode voltage clamp—Potassium currents in oocytes were recorded at room temperature (20–22°C) on Roboocyte2® (Multi Channel Systems) using prepulled and prepositioned intracellular glass microelectrodes with a resistance of 0.3–1 MΩ when filled with 1 M KCl/1.5 M KAc. The bath solution was ND96 (mM: 93.5 NaCl, 2 KCl, 1.8 $CaCl_2$, 2 $MgCl_2$ and 5 Hepes; pH 7.5). Currents were sampled at 5 kHz. For the analysis of channel activation, we kept cells at the holding potential of −90

mV and used 0.5^{-s} depolarizing steps (Δ 10 mV) from −60 mV to +60 mV, followed by a step to −90 mV for 0.5 s to analyze tail currents.

Data analysis—Voltage clamp recordings were analyzed using Roboocyte2+ (Multi Channel Systems), Clampfit (pClamp 8.2, Axon Instruments), Excel (Microsoft), and Origin (OriginLab Corp.) software. The voltage-dependence of channel activation was derived from tail current amplitudes recorded at −90 mV. A Boltzmann function was fit to the current-voltage relationships, $I(V) - I_{max}/(1 - \exp[(V - V_{0.5})/k]) + C$, where I_{max} is the maximum tail current amplitude at test potential V, $V_{0.5}$ the half-maximal activation potential, k a slope factor reflecting characteristics of voltage-dependent channel gating and C a constant. Maximum current amplitudes were compared at the end of a 0.5-s test pulse to −60 mV. All data are shown as mean values ± s.e.m. Statistical analysis was performed with GraphPad Software, and significant differences ($P < 0.05$) determined using Student's *t*-test or Mann-Whitney *U* test.

Western blot—For Western blots, injected *Xenopus* oocytes were lysed in the buffer containing in mM: 20 Tris, 100 NaCl, 1 EDTA, 0.5% Triton X-100, and 10% glycerol with protease inhibitors cOmplete (Roche). Upon determining the protein concentrations (BCA system, Thermo Fisher Scientific), 20 μg of protein was separated by SDS-PAGE on 8% polyacrylamide gels. The proteins were transferred onto nitrocellulose membrane (Whatman, GE Healthcare Europe) and Western blotting performed using a mouse monoclonal antibody to DDK-tag (1:1500; OriGene Technologies, TA50011). Chemiluminescence detection was done according to the manufacturer's protocol (ECL Western Detection Kit; Amersham Pharmacia Biotech Europe). Actin was used as a loading control.

Supplementary Material

Refer to Web version on PubMed Central for supplementary material.

Authors

Mikko Muona[1,2,3,4], Samuel F Berkovic[5], Leanne M Dibbens[6], Karen L Oliver[5], Snezana Maljevic[7], Marta A Bayly[6], Tarja Joensuu[2,3,4], Laura Canafoglia[8], Silvana Franceschetti[8], Roberto Michelucci[9], Salla Markkinen[2,3,4], Sarah E Heron[6], Michael S Hildebrand[5], Eva Andermann[10], Frederick Andermann[10], Antonio Gambardella[11], Paolo Tinuper[9,12], Laura Licchetta[9,12], Ingrid E Scheffer[5,13,14], Chiara Criscuolo[15], Alessandro Filla[15], Edoardo Ferlazzo[16,17], Jamil Ahmad[18], Adeel Ahmad[19], Betul Baykan[20,21], Edith Said[22,23], Meral Topcu[24], Patrizia Riguzzi[9], Mary D King[25,26], Cigdem Ozkara[27], Danielle M Andrade[28], Bernt A Engelsen[29,30], Arielle Crespel[31], Matthias Lindenau[32], Ebba Lohmann[32,34], Veronica Saletti[35], João Massano[36,37], Michael Privitera[38], Alberto J Espay[39], Birgit Kauffmann[40], Michael Duchowny[41,42], Rikke S Møller[43,44], Rachel Straussberg[45,46], Zaid Afawi[46,47], Bruria Ben-Zeev[46,48], Kaitlin E Samocha[49,50,51,52], Mark J Daly[49,50,51], Steven Petrou[13,53], Holger Lerche[7], Aarno Palotie[1,49,50,51,54,55,56], and Anna-Elina Lehesjoki[2,3,4]

Affiliations

[1]Institute for Molecular Medicine Finland, University of Helsinki, Helsinki, Finland [2]Folkhälsan Institute of Genetics, Helsinki, Finland [3]Neuroscience Center, University of Helsinki, Helsinki, Finland [4]Research Program's Unit, Molecular Neurology, University of Helsinki, Helsinki, Finland [5]Epilepsy Research Center, Department of Medicine, University of Melbourne, Austin Health, Heidelberg, Victoria, Australia [6]School of Pharmacy and Medical Sciences, University of South Australia, Adelaide, Australia [7]Department of Neurology and Epileptology, Hertie Institute for Clinical Brain Research, University of Tübingen, Tübingen, Germany [8]Department of Neurophysiopathology, C. Besta Foundation Neurological Institute IRCCS, Milan, Italy [9]IRCCS - Institute of Neurological Sciences of Bologna, Neurology Unit, Bellaria Hospital, Bologna, Italy [10]Montreal Neurological Institute, McGill University, Montreal, Quebec, Canada [11]Institute of Neurology, University Magna Graecia, Catanzaro, Italy [12]Department of Biomedical and Neuromotor Sciences, University of Bologna, Bologna, Italy [13]The Florey Institute of Neuroscience and Mental Health, University of Melbourne, Victoria, Australia [14]Department of Pediatrics, Royal Children's Hospital, University of Melbourne, Victoria, Australia [15]Department of Neurosciences, Reproductive Sciences and Odontostomatology, Federico II University, Naples, Italy [16]Magna Graecia University, Catanzaro, Italy [17]Regional Epilepsy Center, Bianchi-Melacrino-Morelli Hospital, Reggio Calabria, Italy [18]Department of Biotechnology and Informatics, Balochistan University of Information Technology, Engineering and Management Sciences, Quetta, Pakistan [19]Department of Medicine, Mayo Hospital, Lahore, Pakistan [20]Department of Neurology, Istanbul Faculty of Medicine, Istanbul University, Istanbul, Turkey [21]Epilepsy Center (EPIMER), Istanbul University, Istanbul, Turkey [22]Department of Anatomy & Cell Biology, University of Malta, Msida, Malta [23]Section of Medical Genetics, Mater dei Hospital, Msida, Malta [24]Division of Pediatric Neurology, Department of Pediatrics, Hacettepe University Faculty of Medicine, Ankara, Turkey [25]Department of Neurology, Temple Street Children's University Hospital, Dublin, Ireland [26]Academic Centre on Rare Diseases, School of Medicine and Medical Science, University College Dublin, Dublin, Ireland [27]Department of Neurology, Cerrahpasa Medical Faculty, Istanbul University, Istanbul, Turkey [28]Division of Neurology, Department of Medicine, University of Toronto, Toronto Western Hospital, Krembil Neurosciences Program, Toronto, Canada [29]Department of Clinical Medicine, University of Bergen, Bergen, Norway [30]Department of Neurology, Haukeland University Hospital, Bergen, Norway [31]Epilepsy Unit, Hôpital Gui de Chauliac, Montpellier, France [32]Department of Neurology and Epileptology, Epilepsy Center Hamburg-Alsterdorf, Hamburg, Germany [33]Department of Neurodegenerative Diseases, Hertie Institute for Clinical Brain Research, University of Tübingen, Tübingen, Germany [34]DZNE, German Center for Neurodegenerative Diseases, Tübingen, Germany [35]Developmental Neurology Unit, C. Besta Foundation Neurological Institute IRCCS, Milan, Italy [36]Department of Neurology, Centro Hospitalar São João, Porto, Portugal [37]Department of Clinical Neurosciences and Mental Health, Faculty of Medicine,

University of Porto, Porto, Portugal [38]Epilepsy Center, University of Cincinnati Neuroscience Institute, Cincinnati, Ohio, USA [39]Gardner Center for Parkinson disease and Movement Disorders, University of Cincinnati, Cincinnati, Ohio, USA [40]Klinikum Links der Weser, Bremen, Germany [41]Brain Institute, Miami Children's Hospital, Miami, Florida, USA [42]Department of Neurology, University of Miami Miller School of Medicine, Miami, Florida, USA [43]Danish Epilepsy Centre, Dianalund, Denmark [44]Institute of Regional Health Services Research, University of Southern Denmark, Odense, Denmark [45]Neurogenetic Clinic, Child Neurology Institute, Schneider Children's Medical Center of Israel, Petah Tiqvah, Israel [46]Sackler School of Medicine, Tel-Aviv University, Ramat Aviv, Israel [47]Zlotowski Center for Neuroscience, Ben-Gurion University, Israel [48]Pediatric Neurology Unit, Edmond and Lilly Safra Children's Hospital, Sheba Medical Center, Ramat-Gan, Israel [49]Analytic and Translational Genetics Unit, Department of Medicine, Massachusetts General Hospital and Harvard Medical School, Boston, MA, USA [50]Program in Medical and Population Genetics, Broad Institute of Harvard and Massachusetts Institute of Technology, Cambridge, MA, USA [51]Stanley Center for Psychiatric Research, Broad Institute of Harvard and Massachusetts Institute of Technology, Cambridge, MA, USA [52]Program in Genetics and Genomics, Biological and Biomedical Sciences, Harvard Medical School, Boston, MA, USA [53]The Centre for Neural Engineering, University of Melbourne, Victoria, Australia [54]Wellcome Trust Sanger Institute, Wellcome Trust Genome Campus, Hinxton, UK [55]Psychiatric & Neurodevelopmental Genetics Unit, Department of Psychiatry, Massachusetts General Hospital, Boston, MA, USA [56]Department of Neurology, Massachusetts General Hospital, Boston, MA, USA

Acknowledgements

We thank the patients and family members that have contributed samples for the purpose of this study. We also thank the following for patient referrals: K. Joost, K. Carvalho, C. Marques Lourenco, P. Cossette, A. Covanis, A. Parmeggiani, P. Van Bogaert, S. Mole, A. Sierra Marcos, M. Carreno, and S.S. Rich. P. Hakala, E. Hämäläinen, B. Johns, R. Schulz, J. Damiano, H. Löffler, and N. Jezutkovic are thanked for sample logistics and technical assistance in the laboratory, C. Scott and J. Durham (Wellcome Trust Sanger Institute) for exome sequence processing, P. Gormley, B. Winsvold and P. Palta for assistance in exome data analysis, and A. Farooq Bazai for support. CSC – IT Center for Science Ltd. is acknowledged for the allocation of computational resources.

This study was supported by the Folkhälsan Research Foundation (A-E.L.), the Academy of Finland grant no. 141549 (A-E.L.), Wellcome Trust grants [089062] and [098051] (A.P.), the European Commission FP7 projects no. 201413 ENGAGE (A.P.), project no. 242167 SynSys (A.P.), Health-2010 -projects no. 261433 BioSHare (A.P.) and project no. 261123 gEUVADIS (A.P.), the Academy of Finland grants no. 251704 and 263401 (A.P.), the Sigrid Juselius Foundation (A.P.), NIH/RFA-HL-12-007 (A.P.), Emil Aaltonen Foundation (M.M.), Epilepsiatutkimussäätiö (M.M.), University of Helsinki Funds (M.M.), Doctoral Programme in Biomedicine (M.M.), National Health and Medical Research Council (NHMRC) of Australia Program Grant ID 628952 (S.F.B., L.M.D., I.E.S.), NHMRC Career Development Fellowship 1032603 (L.M.D.), NHMRC Early Career Fellowship 1016715 (S.E.H.), German network for rare diseases of the BMBF, IonNeurONet 01GM1105A (S.Mal., H.L.), EuroEPINOMICS program of the ESF, DFG Le1030/11-1 (H.L., S.Mal.), NHMRC program grant 400121 (S.P.), and NMHRC fellowship 1005050 (S.P.). The Florey Institute of Neuroscience and Mental Health (S.P.) is supported by Victorian State Government infrastructure funds.

References

1. Berkovic SF, Andermann F, Carpenter S, Wolfe LS. Progressive Myoclonus Epilepsies: Specific Causes and Diagnosis. N. Engl. J. Med. 1986; 315:296–305. [PubMed: 3088452]
2. Shahwan A, Farrell M, Delanty N. Progressive myoclonic epilepsies: a review of genetic and therapeutic aspects. Lancet Neurol. 2005; 4:239–248. [PubMed: 15778103]
3. Franceschetti S, et al. Progressive myoclonic epilepsies: definitive and still undetermined causes. Neurology. 2014; 82:405–411. [PubMed: 24384641]
4. Pennacchio LA, et al. Mutations in the Gene Encoding Cystatin B in Progressive Myoclonus Epilepsy (EPM1). Science. 1996; 271:1731–1734. [PubMed: 8596935]
5. Berkovic SF, et al. Array-Based Gene Discovery with Three Unrelated Subjects Shows SCARB2/LIMP-2 Deficiency Causes Myoclonus Epilepsy and Glomerulosclerosis. Am. J. Hum. Genet. 2008; 82:673–684. [PubMed: 18308289]
6. Dibbens LM, et al. SCARB2 mutations in progressive myoclonus epilepsy (PME) without renal failure. Ann. Neurol. 2009; 66:532–536. [PubMed: 19847901]
7. Corbett MA, et al. A mutation in the Golgi Qb-SNARE gene GOSR2 causes progressive myoclonus epilepsy with early ataxia. Am. J. Hum. Genet. 2011; 88:657–663. [PubMed: 21549339]
8. Kollmann K, et al. Cell biology and function of neuronal ceroid lipofuscinosis-related proteins. BBA-Mol. Basis Dis. 2013; 1832:1866–1881. [PubMed: 23402926]
9. Ramachandran N, Girard J-M, Turnbull J, Minassian BA. The autosomal recessively inherited progressive myoclonus epilepsies and their genes. Epilepsia. 2009; 50:29–36. [PubMed: 19469843]
10. Samocha KE, et al. A framework for the interpretation of *de novo* mutation in human disease. Nat. Genet. 2014; 46:944–950. [PubMed: 25086666]
11. Davis RL, et al. Association between conformational mutations in neuroserpin and onset and severity of dementia. Lancet. 2002; 359:2242–2247. [PubMed: 12103288]
12. Hsiao K, et al. Linkage of a prion protein missense variant to Gerstmann-Straussler syndrome. Nature. 1989; 338:342–345. [PubMed: 2564168]
13. Baets J, et al. Mutations in SACS cause atypical and late-onset forms of ARSACS. Neurology. 2010; 75:1181–1188. [PubMed: 20876471]
14. Romano A, et al. Comparative Analysis and Functional Mapping of SACS Mutations Reveal Novel Insights into Sacsin Repeated Architecture. Hum. Mutat. 2013; 34:525–537. [PubMed: 23280630]
15. Synofzik M, et al. Autosomal recessive spastic ataxia of Charlevoix Saguenay (ARSACS): expanding the genetic, clinical and imaging spectrum. Orphanet J. Rare Dis. 2013; 8:41. [PubMed: 23497566]
16. Afawi Z, et al. TBC1D24 mutation associated with focal epilepsy, cognitive impairment and a distinctive cerebro-cerebellar malformation. Epilepsy Res. 2013; 105:240–244. [PubMed: 23517570]
17. Campeau PM, et al. The genetic basis of DOORS syndrome: an exome-sequencing study. Lancet Neurol. 2014; 13:44–58. [PubMed: 24291220]
18. Corbett MA, et al. A Focal Epilepsy and Intellectual Disability Syndrome Is Due to a Mutation in TBC1D24. Am. J. Hum. Genet. 2010; 87:371–375. [PubMed: 20797691]
19. Falace A, et al. TBC1D24, an ARF6-Interacting Protein, Is Mutated in Familial Infantile Myoclonic Epilepsy. Am. J. Hum. Genet. 2010; 87:365–370. [PubMed: 20727515]
20. Guven A, Tolun A. TBC1D24 truncating mutation resulting in severe neurodegeneration. J. Med. Genet. 2013; 50:199–202. [PubMed: 23343562]
21. Harkin LA, et al. The spectrum of SCN1A-related infantile epileptic encephalopathies. Brain. 2007; 130:843–852. [PubMed: 17347258]
22. Claes L, et al. De Novo Mutations in the Sodium-Channel Gene SCN1A Cause Severe Myoclonic Epilepsy of Infancy. Am. J. Hum. Genet. 2001; 68:1327–1332. [PubMed: 11359211]
23. Ried T, et al. Localization of a Highly Conserved Human Potassium Channel Gene (NGK2-KV4; KCNC1) to Chromosome 11p15. Genomics. 1993; 15:405–411. [PubMed: 8449507]

24. Waters MF, et al. Mutations in voltage-gated potassium channel KCNC3 cause degenerative and developmental central nervous system phenotypes. Nat. Genet. 2006; 38:447–451. [PubMed: 16501573]
25. Figueroa KP, et al. KCNC3: phenotype, mutations, channel biophysics—a study of 260 familial ataxia patients. Hum. Mutat. 2010; 31:191–196. [PubMed: 19953606]
26. Figueroa KP, et al. Frequency of KCNC3 DNA Variants as Causes of Spinocerebellar Ataxia 13 (SCA13). PLoS ONE. 2011; 6:e17811. [PubMed: 21479265]
27. Németh AH, et al. Next generation sequencing for molecular diagnosis of neurological disorders using ataxias as a model. Brain. 2013; 136:3106–3118. [PubMed: 24030952]
28. Rudy B, McBain CJ. Kv3 channels: voltage-gated K+ channels designed for high-frequency repetitive firing. Trends Neurosci. 2001; 24:517–526. [PubMed: 11506885]
29. Seoh S-A, Sigg D, Papazian DM, Bezanilla F. Voltage-Sensing Residues in the S2 and S4 Segments of the Shaker K+ Channel. Neuron. 1996; 16:1159–1167. [PubMed: 8663992]
30. Aggarwal SK, MacKinnon R. Contribution of the S4 Segment to Gating Charge in the Shaker K+ Channel. Neuron. 1996; 16:1169–1177. [PubMed: 8663993]
31. Minassian NA, Lin M-CA, Papazian DM. Altered Kv3.3 channel gating in early-onset spinocerebellar ataxia type 13. J. Physiol. 2012; 590:1599–1614. [PubMed: 22289912]
32. Moreau A, Gosselin-Badaroudine P, Chahine M. Biophysics, pathophysiology, and pharmacology of ion channel gating pores. Front. Pharmacol. 2014; 5:53. [PubMed: 24772081]
33. Starace DM, Bezanilla F. Histidine Scanning Mutagenesis of Basic Residues of the S4 Segment of the Shaker K+ Channel. J. Gen. Physiol. 2001; 117:469–490. [PubMed: 11331357]
34. Ho CS, Grange RW, Joho RH. Pleiotropic effects of a disrupted K+ channel gene: Reduced body weight, impaired motor skill and muscle contraction, but no seizures. Proc. Natl. Acad. Sci. U. S. A. 1997; 94:1533–1538. [PubMed: 9037088]
35. Joho RH, Ho CS, Marks GA. Increased gamma- and decreased delta-oscillations in a mouse deficient for a potassium channel expressed in fast-spiking interneurons. J. Neurophysiol. 1999; 82:1855–1864. [PubMed: 10515974]
36. Espinosa F, et al. Alcohol Hypersensitivity, Increased Locomotion, and Spontaneous Myoclonus in Mice Lacking the Potassium Channels Kv3.1 and Kv3.3. J. Neurosci. 2001; 21:6657–6665. [PubMed: 11517255]
37. Issa FA, Mazzochi C, Mock AF, Papazian DM. Spinocerebellar Ataxia Type 13 Mutant Potassium Channel Alters Neuronal Excitability and Causes Locomotor Deficits in Zebrafish. J. Neurosci. 2011; 31:6831–6841. [PubMed: 21543613]
38. Erisir A, Lau D, Rudy B, Leonard CS. Function of specific K(+) channels in sustained high-frequency firing of fast-spiking neocortical interneurons. J. Neurophysiol. 1999; 82:2476–2489. [PubMed: 10561420]
39. Sabatini BL, Regehr WG. Control of Neurotransmitter Release by Presynaptic Waveform at the Granule Cell to Purkinje Cell Synapse. J. Neurosci. 1997; 17:3425–3435. [PubMed: 9133368]
40. Irie T, Matsuzaki Y, Sekino Y, Hirai H. Kv3.3 channels harbouring a mutation of spinocerebellar ataxia type 13 alter excitability and induce cell death in cultured cerebellar Purkinje cells. J. Physiol. 2014; 592:229–247. [PubMed: 24218544]
41. Gan L, Kaczmarek LK. When, where, and how much? Expression of the Kv3.1 potassium channel in high-frequency firing neurons. J. Neurobiol. 1998; 37:69–79. [PubMed: 9777733]
42. Lonsdale J, et al. The Genotype-Tissue Expression (GTEx) project. Nat. Genet. 2013; 45:580–585. [PubMed: 23715323]
43. Wulff H, Castle NA, Pardo LA. Voltage-gated potassium channels as therapeutic targets. Nat. Rev. Drug Discov. 2009; 8:982–1001. [PubMed: 19949402]
44. Kälviäinen R, et al. Clinical picture of EPM1-Unverricht-Lundborg disease. Epilepsia. 2008; 49:549–556. [PubMed: 18325013]
45. Lehtinen MK, et al. Cystatin B Deficiency Sensitizes Neurons to Oxidative Stress in Progressive Myoclonus Epilepsy, EPM1. J. Neurosci. 2009; 29:5910–5915. [PubMed: 19420257]

46. Okuneva O, et al. Abnormal microglial activation in the Cstb−/− mouse, a model for progressive myoclonus epilepsy, EPM1. Glia. 2014 Advance online publication, 18 Oct 2014. DOI 10.1002/glia.22760.
47. Buzzi A, et al. Loss of cortical GABA terminals in Unverricht-Lundborg disease. Neurobiol. Dis. 2012; 47:216–224. [PubMed: 22538221]
48. Joensuu T, et al. Gene expression alterations in the cerebellum and granule neurons of Cstb(−/−) mouse are associated with early synaptic changes and inflammation. PLoS ONE. 2014; 9:e89321. [PubMed: 24586687]
49. Kong A, et al. Rate of de novo mutations and the importance of father's age to disease risk. Nature. 2012; 488:471–475. [PubMed: 22914163]
50. Brooks NL, Corey MJ, Schwalbe RA. Characterization of N-glycosylation consensus sequences in the Kv3.1 channel. FEBS J. 2006; 273:3287–3300. [PubMed: 16792699]
51. Hall MK, Cartwright TA, Fleming CM, Schwalbe RA. Importance of glycosylation on function of a potassium channel in neuroblastoma cells. PLoS ONE. 2011; 6:e19317. [PubMed: 21541302]
52. Bonten E, van der Spoel A, Fornerod M, Grosveld G, d'Azzo A. Characterization of human lysosomal neuraminidase defines the molecular basis of the metabolic storage disorder sialidosis. Genes Dev. 1996; 10:3156–3169. [PubMed: 8985184]
53. Lukong KE, et al. Characterization of the sialidase molecular defects in sialidosis patients suggests the structural organization of the lysosomal multienzyme complex. Hum. Mol. Genet. 2000; 9:1075–1085. [PubMed: 10767332]
54. Canafoglia L, et al. Expanding sialidosis spectrum by genome-wide screening: NEU1 mutations in adult-onset myoclonus. Neurology. 2014; 82:2003–2006. [PubMed: 24808020]
55. Chan EM, et al. Mutations in NHLRC1 cause progressive myoclonus epilepsy. Nat. Genet. 2003; 35:125–127. [PubMed: 12958597]
56. Leutenegger A-L, et al. Estimation of the Inbreeding Coefficient through Use of Genomic Data. Am. J. Hum. Genet. 2003; 73:516–523. [PubMed: 12900793]
57. Purcell S, et al. PLINK: a tool set for whole-genome association and population-based linkage analyses. Am. J. Hum. Genet. 2007; 81:559–575. [PubMed: 17701901]
58. Li H, Durbin R. Fast and accurate short read alignment with Burrows-Wheeler transform. Bioinformatics. 2009; 25:1754–1760. [PubMed: 19451168]
59. McKenna A, et al. The Genome Analysis Toolkit: A MapReduce framework for analyzing next-generation DNA sequencing data. Genome Res. 2010; 20:1297–1303. [PubMed: 20644199]
60. DePristo MA, et al. A framework for variation discovery and genotyping using next-generation DNA sequencing data. Nat. Genet. 2011; 43:491–498. [PubMed: 21478889]
61. McLaren W, et al. Deriving the consequences of genomic variants with the Ensembl API and SNP Effect Predictor. Bioinformatics. 2010; 26:2069–2070. [PubMed: 20562413]
62. Benson G. Tandem repeats finder: a program to analyze DNA sequences. Nucleic Acids Res. 1999; 27:573–580. [PubMed: 9862982]
63. Kent WJ, et al. The Human Genome Browser at UCSC. Genome Res. 2002; 12:996–1006. [PubMed: 12045153]
64. Kircher M, et al. A general framework for estimating the relative pathogenicity of human genetic variants. Nat. Genet. 2014; 46:310–315. [PubMed: 24487276]
65. Adzhubei IA, et al. A method and server for predicting damaging missense mutations. Nat. Methods. 2010; 7:248–249. [PubMed: 20354512]
66. Kumar P, Henikoff S, Ng PC. Predicting the effects of coding non-synonymous variants on protein function using the SIFT algorithm. Nat. Protoc. 2009; 4:1073–1081. [PubMed: 19561590]
67. Schwarz JM, Rodelsperger C, Schuelke M, Seelow D. MutationTaster evaluates disease-causing potential of sequence alterations. Nat. Methods. 2010; 7:575–576. [PubMed: 20676075]
68. Liu X, Jian X, Boerwinkle E. dbNSFP v2.0: A Database of Human Non-synonymous SNVs and Their Functional Predictions and Annotations. Hum. Mutat. 2013; 34:E2393–E2402. [PubMed: 23843252]
69. The 1000 Genomes Consortium. An integrated map of genetic variation from 1,092 human genomes. Nature. 2012; 491:56–65. [PubMed: 23128226]

70. Browning BL, Browning SR. Improving the Accuracy and Efficiency of Identity-by-Descent Detection in Population Data. Genetics. 2013; 194:459–471. [PubMed: 23535385]
71. Robinson JT, et al. Integrative genomics viewer. Nat. Biotechnol. 2011; 29:24–26. [PubMed: 21221095]
72. Hamosh A, Scott AF, Amberger JS, Bocchini CA, McKusick VA. Online Mendelian Inheritance in Man (OMIM), a knowledgebase of human genes and genetic disorders. Nucleic Acids Res. 2005; 33:D514–D517. [PubMed: 15608251]
73. Lemke JR, et al. Targeted next generation sequencing as a diagnostic tool in epileptic disorders. Epilepsia. 2012; 53:1387–1398. [PubMed: 22612257]
74. Petrovski S, Wang Q, Heinzen EL, Allen AS, Goldstein DB. Genic Intolerance to Functional Variation and the Interpretation of Personal Genomes. PLoS Genet. 2013; 9:e1003709. [PubMed: 23990802]
75. Fuentes Fajardo KV, et al. Detecting false-positive signals in exome sequencing. Hum. Mutat. 2012; 33:609–613. [PubMed: 22294350]
76. The UniProt Consortium. Activities at the Universal Protein Resource (UniProt). Nucleic Acids Res. 2014; 42:D191–D198. [PubMed: 24253303]
77. Shoffner JM, et al. Myoclonic epilepsy and ragged-red fiber disease (MERRF) is associated with a mitochondrial DNA tRNA(Lys) mutation. Cell. 1990; 61:931–937. [PubMed: 2112427]
78. Ye J, et al. Primer-BLAST: A tool to design target-specific primers for polymerase chain reaction. BMC Bioinformatics. 2012; 13:134. [PubMed: 22708584]
79. Gu Y, Barry J, McDougel R, Terman D, Gu C. Alternative Splicing Regulates Kv3.1 Polarized Targeting to Adjust Maximal Spiking Frequency. J. Biol. Chem. 2012; 287:1755–1769. [PubMed: 22105078]

Europe PMC Funders Author Manuscripts

Europe PMC Funders Author Manuscripts

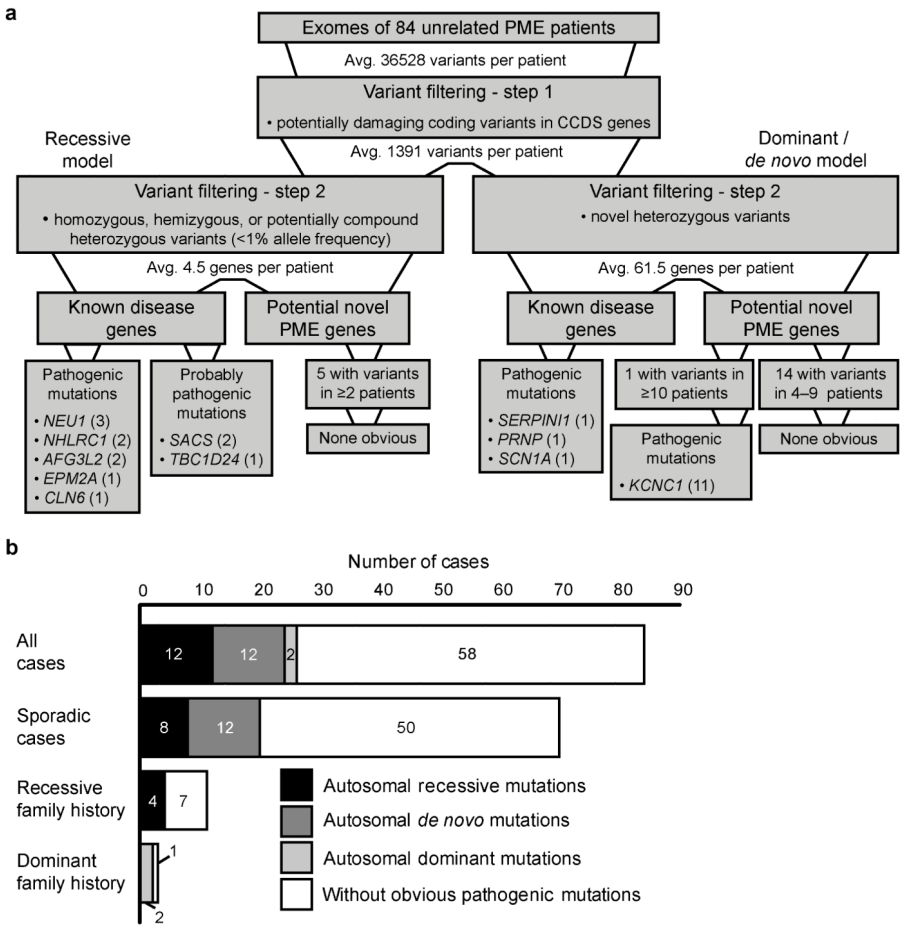

Figure 1.

Analysis of the PME exomes. **(a)** A simplified flow chart of the exome data analysis strategy under autosomal and sex-linked recessive and dominant/*de novo* inheritance models, and summary of results. The average total number of variants per exome (36528) refers to single nucleotide variants and indels passing quality filtering within the exome bait regions. Numbers in parentheses after gene names indicate numbers of patients with mutations in the gene. Gene and patient counts under 'Potential novel PME genes' are derived after excluding patients with pathogenic or probably pathogenic mutations in known disease genes or with the pathogenic mutation in *KCNC1* identified in this study. **(b)** Numbers and proportions of patients without obvious pathogenic mutations or with pathogenic or probably pathogenic mutations of variable patterns of inheritance. The three patients with probably pathogenic mutations are included under sporadic cases with recessive mutations. Case PME84-1 with the recurrent *de novo KCNC1* mutation is included under cases with autosomal dominant mutations with a dominant family history (Fig. 2a).

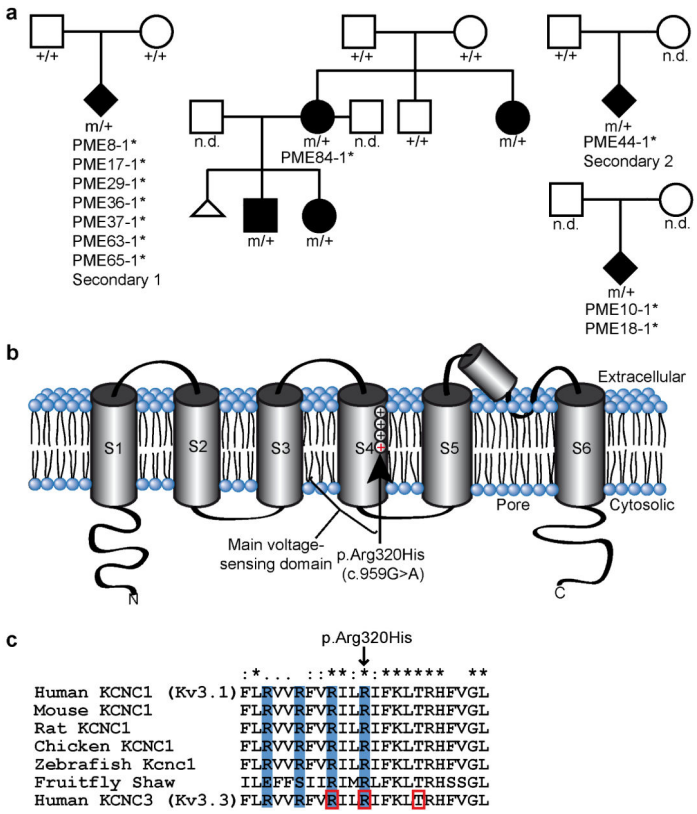

Figure 2.

The recurrent c.959G>A mutation in *KCNC1*. **(a)** Pedigrees of 13 unrelated patients demonstrate the *de novo* occurrence of the c.959G>A mutation in *KCNC1*. Patient IDs of the exome-sequenced cases are marked with asterisks. Triangle symbol indicates miscarriage at 8 weeks. m, c.959G>A; +, wild-type; n.d., not determined. **(b)** A cartoon showing the domain structure of a single $K_V3.1$ subunit. The positively charged arginine residues (marked with "+") in the S4 segment detect changes in voltage. The p.Arg320His changes one of the arginine residues to a histidine (red "+"and arrow). **(c)** ClustalX amino acid sequence comparison of the voltage-sensing S4 segment shows full conservation of the arginine 320 (indicated by an arrow) across different species. The four positively charged arginine residues (Arg311, Arg314, Arg317, Arg320) occurring every third position are highlighted in blue. The $K_V3.3$ residues Arg420, Arg423, Thr428, mutated in spinocerebellar ataxia[24,25,27], are in red boxes. Asterisks, colons, and periods indicate fully conserved, strongly similar, and weakly similar residues, respectively.

Europe PMC Funders Author Manuscripts

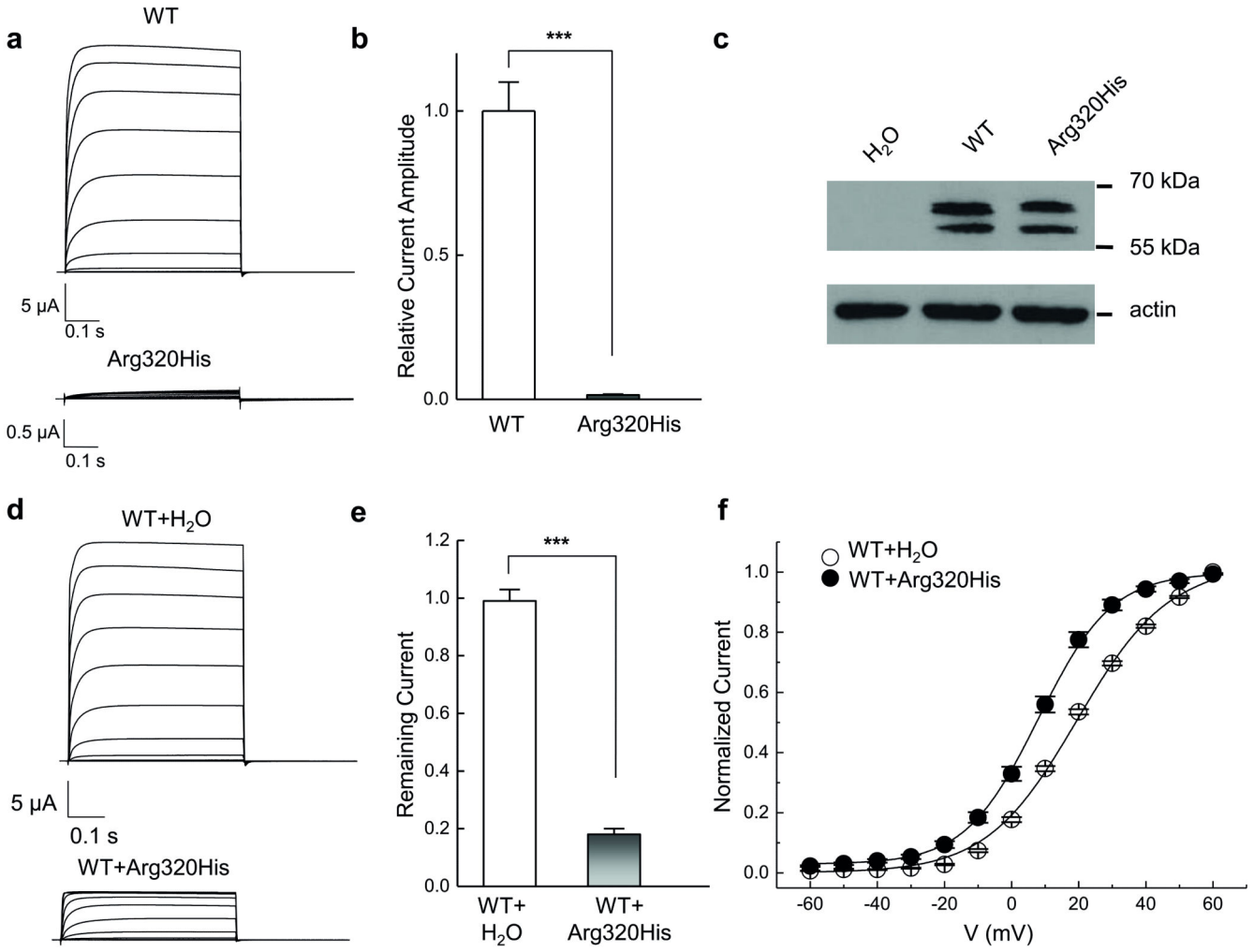

Figure 3.

Functional analysis of p.Arg320His in $K_V3.1$. **(a)** Representative traces of whole-cell currents recorded in *Xenopus laevis* oocytes, injected with the same amount of cRNA encoding $K_V3.1$ wild-type (WT) or Arg320His, during 0.5 s voltage steps ranging from −60 mV to +60 mV. **(b)** Current amplitudes analyzed at the end of the voltage step to +60 mV and normalized to the mean current amplitude of WT (n = 49) recorded on the same day, revealed significantly smaller potassium currents for the Arg320His (n = 50) (Mann-Whitney *U* test; ***$P < 0.001$). **(c)** Western blot analysis of *Xenopus laevis* oocytes injected with either WT or Arg320His mutant cRNA using a mouse antibody to DDK-tag showed similar bands in total cell lysates in the two representative experiments. H_2O-injected oocytes were used as a negative control and actin served as a loading control. The presence of two bands in the blot is likely to be due to N-glycosylation that the $K_V3.1$ protein (expected protein size ~56kDa) is subjected to *in vivo* and in heterologous expression systems[50,51]. **(d)**,**(e)** A dominant-negative effect of Arg320His mutant on WT channels was determined when a constant amount of the WT cRNA was injected with either H_2O or the same amount of Arg320His cRNA in a 1:1 ratio. **(d)** Representative whole-cell currents recorded as in **a** were decreased for the co-expression of WT and Arg320His mutant

channels. **(e)** Analysis of current amplitudes at the end of a 0.5-s pulse to +60 mV, followed by normalization to the WT recorded on the same day, revealed that the co-expression with the Arg320His mutant (n = 27) reduced currents by about 4-fold compared to the WT (n = 32) (Student's *t*-test; ***$P < 0.001$). **(f)** Current-voltage relationships of WT and co-expression of WT with Arg320His channels revealed a leftward shift for the latter, resulting in a significant increase of normalized tail current amplitudes in almost the whole range of analyzed potentials (Student's *t*-test; $P < 0.001$ for −60 mV to +50 mV). Lines represent fits of a Boltzmann function. The $V_{0.5}$ was 19.6 ± 0.5 mV (n = 19) and 8.0 ± 1.3 mV (n = 16) (Student's *t*-test; $P < 0.001$) and the slope factor *k* 12.9 ± 0.2 and 10.2 ± 0.3 (Student's *t*-test; $P < 0.001$) for WT and WT/Arg320His co-expression, respectively. Data in **b**,**e**,**f** are presented as means ± s.e.m.

Europe PMC Funders Author Manuscripts

Europe PMC Funders Author Manuscripts

Table 1

Clinical features of patients with the c.959G>A mutation (p.Arg320His) in *KCNC1*

Individual ID	Ancestry	Gender	Onset age	Initial symptom	Seizures		Learning disability	Cognitive decline	Age and outcome
					Myoclonus	Tonic-clonic			
Exome sequenced patients									
PME8-1	Italian	M	12y	Myoclonus	+++	+	No	Yes	38y; Wheelchair at 27y
PME10-1	Italian	M	6y	Myoclonus	+++	++	No	Possible	34y; Wheelchair at 17y
PME17-1	French	M	<5y	Ataxia	+++	++	No	No	40y; Wheelchair at 16y
PME18-1	Norwegian	F	10y[§]	Myoclonus	+++	+	No	Yes	36y; Wheelchair at 15y
PME29-1	German	M	9y	Tremor/Myoclonus	++	+	Yes	No	24y; Cautiously ambulant
PME36-1	American (Italian)	F	7y	Tremor	+++	+	No	No	22y; Wheelchair at 14y
PME37-1	Italian	F	10y	Myoclonus	+++	+	No	No	19y; Wheelchair at 17y
PME44-1	French Canadian	F	12y	Myoclonus	++	+	No	Yes	24y; Walker at 17y
PME63-1	Moldavian[☼]	F	9y	Myoclonus	+++	++	No	Possible[¶]	15y; Wheelchair at 13y
PME65-1	Portuguese	F	9y	Myoclonus	+++	+	No	Yes	25y; Wheelchair at 19y
PME84-1	Israeli (Sephardic)	F	10y	Tremor	+	+	Yes	No	42y; Ambulant
Sanger sequenced patients									
PME84-sister	Israeli (Sephardic)	F	13y	Myoclonus	++	++	Yes	Yes	37y; Cautiously ambulant
PME84-son	Israeli (Sephardic)	M	12y	Ataxia	+	+	Yes	Yes	19y; Cautiously ambulant
PME84-daughter	Israeli (Sephardic)	F	14y	Tonic-clonic seizure	−	+	Yes	No	16y; Ambulant
Secondary 1	Danish	M	10y[‡]	Myoclonus	++	+	No	Yes	18y; Cautiously ambulant
Secondary 2[†]	Israeli	M	n/a	n/a	n/a	n/a	n/a	n/a	n/a

+ (mild), ++ (moderate), +++ (severe), − (not observed)

[§] earlier absence seizures

[☼] ascertained in Italy

[¶] severe myoclonus and language barrier prevented good assessment

[‡] simple febrile seizures at 6 - 12 months

[†] no detailed clinical data available

Europe PMC Funders Author Manuscripts

Table 2

Pathogenic or probably pathogenic mutations in known PME, epilepsy or neurodegenerative disease associated genes

		Patient ID, gender	Gene	Zygosity	Coding DNA change[§]	Protein change[§]	CADD, SIFT, PolyPhen, Mutation taster prediction[‡]	Allele frequency in 1000G/EVS[✡] (%)	Previously reported pathogenic mutation (reference)	Disease associated to the gene (OMIM gene number)
Recessive	Pathogenic	PME23-1, F	*NEU1*	het	c.1208delG	p.Ser403ThrfsTer85	32,NA,NA,NA	0/0	Yes[52]	PME: sialidosis (608272)
				het	c.982G>A	p.Gly328Ser	32,D,D,D	0/0	Yes[53]	
		PME51-1, F	*NEU1*	het	c.982G>A	p.Gly328Ser	32,D,D,D	0/0	Yes[53]	
				het	c.679G>A	p.Gly227Arg	28.5,D,D,D	0/0	Yes[53]	
		PME87-1, F	*NEU1*	het	c.914G>A	p.Arg305His	9.4,B,PD,D	0/0	No, but p.Arg305Cys is reported[54]	
				het	c.625delG	p.Glu209SerfsTer94	26.1,NA,NA,NA	0/0	Yes[53]	
		PME35-1, F	*NHLRC1*	hom	c.436G>A	p.Asp146Asn	15.75,B,PD,D	0/0	Yes[55]	PME: Lafora disease (608072)
		PME81-1, M	*NHLRC1*	hom	c.830C>A	p.Ala277Glu	12.72,D,D,D	0/0	No	
		PME82-1, M	*EPM2A*	hom	c.590A>T	p.Asp197Val	27.4,D,D,D	0/0	No	PME: Lafora disease (607566)
		PME33-1, M	*CLN6*	hom	c.509A>G	p.Tyr170Cys	17.11,D,D,D	0/0	No	PME: Neuronal ceroid lipofuscinosis, late infantile and adult variants (606725)
		PME62-1, M	*AFG3L2*	hom	c.1875G>A	p.Met625Ile	30,B,PD,D	0/0	No	Spinocerebellar ataxia 28 and spastic ataxia with PME (604581)
		PME32-1, F	*AFG3L2*	hom	c.1875G>A	p.Met625Ile	30,B,PD,D	0/0	No	
	Probably pathogenic	PME14-1, F	*TBC1D24*	hom	c.1079G>T	p.Arg360Leu	19.83,D,D,D	0/0	No	Multiple neurological diseases including familial infantile myoclonic epilepsy (613577). PME not previously described
		PME15-1, F	*SACS*	het	c.8393C>A	p.Pro2798Gln	25.7,D,D,D	0.09%/0.29%	Possible[13¶]	Autosomal Recessive Spastic Ataxia of the Charlevoix Saguenay (604490). PME not previously described
				het	c.2996T>C	p.Ile999Thr	17.35,D,B,D	0/0.015%	No	
		PME75-1, F	*SACS*	het	c.8393C>A	p.Pro2798Gln	25.7,D,D,D	0.09%/0.29%	Possible[13¶]	
				het	c.1373C>T	p.Thr458Ile	17.45,D,D,D	0.14%/0.24%	Possible[15¶] and yes[14]	
Dominant/*de novo*	Pathogenic	PME42-1, F	*SERPINI1*	het	c.1175G>A	p.Gly392Glu	22.5,D,D,D	0/0	Yes[11]	PME: Familial encephalopathy with neuroserpin inclusion bodies (604218)
		PME86-1, F	*PRNP*	het	c.305C>T	p.Pro102Leu	19.12,D,D,D	0/0	Yes[12]	Gerstmann-Sträussler-Scheinker disease (176640). PME not previously described
		PME20-1, F	*SCN1A*	het	c.677C>T	p.Thr226Met	20.5,D,D,D	0/0	Yes[21]	Dravet syndrome (182389)

[§]Genomic positions and more detailed annotations of the mutations are presented in Supplementary Table 3. Mutation coding DNA nucleotide and amino acid position numbers are based on Ensembl transcripts listed under Accession codes.

Europe PMC Funders Author Manuscripts

‡CADD scores of >15 indicate deleteriousness of the variant (see Online Methods). B=benign (not considered deleterious by the method), PD=possibly deleterious (applies to PolyPhen only), D=deleterious, NA=not available.

✡1000G, 1000 Genomes project; EVS, Exome Variant Server of NHLBI Exome Sequencing Project.

¶See Supplementary Note for discussion of the pathogenicity of the previously reported SACS mutations.